molecular pharmaceutics

Article

Dual-stimuli responsive supramolecular self-assemblies based on the host-guest interaction between #-cyclodextrin and azobenzene for cellular drug release

JianGuo Zhang, Zi-Hao Zhou, Lin Li, Yan-Ling Luo, Feng Xu, and Yashao Chen

Mol. Pharmaceutics, **Just Accepted Manuscript** • DOI: 10.1021/acs.molpharmaceut.9b01142 • Publication Date (Web): 03 Mar 2020

Just Accepted

is published by the American Chemical Society. 1155 Sixteenth Street N.W., Washington, DC 20036

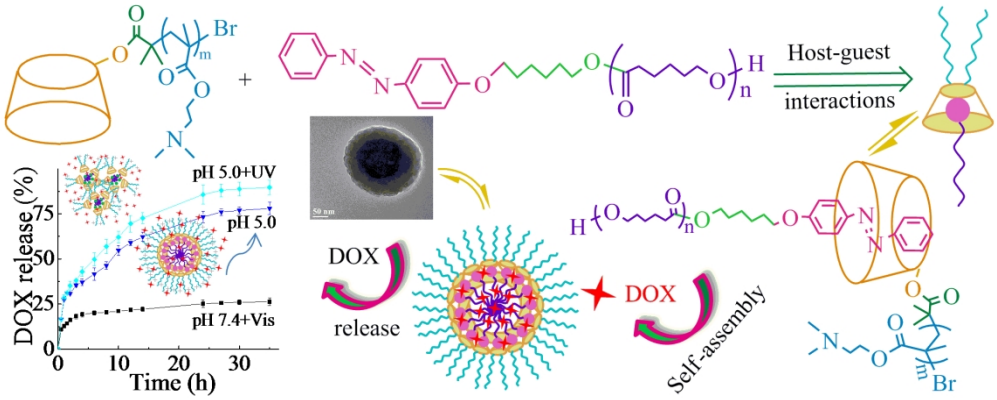

Revised Graphical Abstract

178x71mm (300 x 300 DPI)

Dual-stimuli responsive supramolecular self-assemblies based on the host-guest interaction between β-cyclodextrin and azobenzene for cellular drug release

JianGuo Zhang[§], Zi-Hao Zhou[§], Lin Li[§], Yan-Ling Luo*, Feng Xu*, Yashao Chen

Key Laboratory of Macromolecular Science of Shaanxi Province, School of Chemistry and Chemical Engineering, Shaanxi Normal University, Xi'an 710062, P.R. China

[§] JianGuo Zhang, Zi-Hao Zhou and Lin Li contributed equally to this work.

Corresponding authors' details:

Yan-Ling Luo and Feng Xu

Fax: +86 29 81530727.

E-mail addresses: luoyanl@snnu.edu.cn (Y. L. Luo) and fengxu@snnu.edu.cn (F. Xu).

Affiliation: Key Laboratory of Macromolecular Science of Shaanxi Province, School of Chemistry & Chemical Engineering, Shaanxi Normal University, Xi'an 710062, People's Republic of China.

Abstract

Health has always been a hot topic of concern, whereas cancer is one of the largest security risks to human health. Although the existing drug delivery systems (DDSs) have been extensively reported and commercially applied, there are still some issues that have yet to be well-resolved, including the toxicity, side-effects and targeted therapy efficiency of drugs. Consequently, it is still necessary to develop a novel, highly efficient, controlled and targeted DDS for cancer therapy. For this, a supramolecular polymer, β-CD-g-PDMAEMA@Azo-PCL, was designed and developed through the host-guest inclusion complexation interactions between a host polymer, β-cyclodextrin-*graft*-poly(2-(dimethylamino)ethyl methacrylate) (β-CD-*g*-PDMAEMA), and a guest polymer, azobenzene modified poly(ε-caprolactone) (Azo-PCL), and was characterized by various analysis techniques. The supramolecular assembly was examined in various pH environments and/or under UV-vis irradiation, showing the formation of supramolecular assemblies from regular spherical shapes to irregular aggregates with various hydrodynamic diameters. The 2D NOESY NMR studies showed the formation of inclusion complexation between Azo-PCL and β-CD-*g*-PDMAEMA and between β-CD and the side groups of PDMAEMA. The supramolecular assemblies could encapsulate doxorubicin to form spherical core-shell drug-carrying micelles with an entrapment efficiency of 66.1%. The effects of external environment stimuli on the *in vitro* drug release were investigated, showing light- and pH-modulated drug release properties. The cytotoxicity assessment indicated that the blank supramolecular micelles were nontoxic, whereas the drug-loaded micelles exhibited comparable or even superior anticancer activity to the anticancer activity of free DOX and inhibition of cancer cell proliferation. Therefore, the developed

supramolecular assemblies can potentially be used as drug controlled release carriers.

Keywords: β-Cyclodextrin, Azobenzene, Host-guest interactions, Stimulus responsiveness

1. Introduction

In recent years, supramolecular polymers have attracted extensive attention due to their potential applications in the fields of biotechnology, nanosensing, drug delivery and gene diagnosis and treatment [1-5]. Supramolecular micelles formed by the self-assembly of polymers usually take on regular spherical core-shell structures. Their hydrophobic cores can interact with therapeutic drugs physically or chemically, thus serving as nanoscale containers for encapsulating hydrophobic drugs, while the hydrophilic shells can interact with solvents to improve the micelle stability and prolong the blood circulation time [2-4]. This class of supramolecular polymers is highly oriented and bound together by non-covalent weak interactions, such as multiple hydrogen bonds, host-guest interactions, π-π stacking, metal coordination bonds and electrostatic interactions [1,2,5]. Among them, the host-guest interactions have selective recognizability and abundant responsivity to stimuli. Host-guest molecules are combined by hydrophobic interactions due to their complementary characteristics in size and structure, which provides a broad space for the development and application of various intelligent materials [1-5].

β-cyclodextrin (β-CD) is a natural macrocyclic oligosaccharide composed of seven D-galactose units connected by 1,4-glycoside bonds, with a truncated pyramidal cavity structure of hydrophilic outer margins and hydrophobic inner cavities [6,7]. Its unique molecular structure enables it to complex with a variety of organic compounds, which in turn increases the solubility of hydrophobic drugs, enhances the stability and bioavailability of drugs, and reduces the systemic toxicity of drugs; moreover its low cost, good biocompatibility and biodegradability make it the most widely used host molecule to build supramolecular polymers. Composite micelles with recognizability,

reversibility and controllability can be prepared by means of the host-guest interaction between β-CD and hydrophobic molecules, which provides more possibilities for the synthesis of anticancer drug carriers. Kang et al prepared a nano-self-assembly with both thermal and redox responsiveness [8]. Gao et al synthesized a supramolecular system by noncovalent coupling, which could further self-assemble into nanorods with good thermal response and fluorescence properties [9].

Compared with traditional polymers, supramolecular polymers can be joined together through reversible and dynamic noncovalent interactions, which makes supramolecular polymer materials have a strong stimulus response performance [10,11]. Supramolecular polymers can have an autonomous response to intracellular environmental stimuli, including the pH, temperature, redox potential, enzymes, glucose, ionic strength, etc., and external environmental stimuli (including light, electricity, magnetism, ultrasound, etc.), to further improve the therapeutic effect of hydrophobic drugs on tumor tissues and minimize the damage to healthy cells [12]. A light stimulus is widely used in clinical treatment due to its characteristics of cleanness, flexibility, controllability, non-contact and low cost [13]. Polymers with photoresponse performance can convert light signals to chemical signals through photochemical reactions when the photosensitive groups in the molecule are stimulated by light, thus resulting in changes in the structure, polarity, solubility, and aggregation behavior of the polymers [14]. Azobenzene (Azo) contains a large conjugated system and is a typical photoresponsive group. Azo can change from the trans-configuration to the cis-configuration under UV irradiation, whereas it can reversibly change from the cis-configuration to the trans-configuration under visible light irradiation, which makes the supramolecular polymers containing azo units reversibly self-assemble/dissociate

under alternating UV and visible light irradiation [15-17]. By means of hydrophobic interactions and intermolecular van der Waals forces, trans-azobenzene can smoothly enter into the cavity of β-CD and undergo complexation. However, cis-azobenzene does not match the structure of β-CD and cannot form complexes. Therefore, cis-azobenzene is an "active" unit, and trans-azobenzene is an "inactive" unit for drug delivery and release systems [18,19]. Furthermore, the isomerization amount of azobenzene is proportional to the UV emission energy, and hence, the controlled release of drugs can be realized by adjusting the lighting time [20]. Wang et al designed a novel *in vivo* drug delivery system by combining photodynamic therapy with hypoxic-responsive chemotherapy [21]. Gao et al synthesized a photoresponsive supramolecular polymer brush by means of the host-guest interaction between β-CD and azobenzene, which provides a new platform for the synthesis of self-assemblies with different sizes [22]. Bian et al offered a reusable photo-responsive surface based on host-guest interactions between azobenzene and β-CD for specific cell-controlled release *via* alternating UV and visible light irradiation [23]. Yang et al reported a photo- and temperature-responsive amphiphilic block copolymer micelle assembly, poly(N-isopropylacrylamide)-block-poly-(2-nitrobenzyl methacrylate), for the controlled release of hydrophobic guest molecules [24]. These novel findings afford a new choice for the isolation and analysis of cancer cells, particularly for the controlled release of anticancer drugs.

On the other hand, the pH of tumor microenvironments (6.5~7.0) is slightly lower than that of normal human tissues (approximately 7.4) due to the rapid growth of tumor cells and vigorous anaerobic metabolism, which produces a large number of acid metabolites such as lactic acid [25]. If pH responsive functional groups are

integrated into the supramolecular polymers, the hydrophilic/hydrophobic balance of polymer chains can be changed by adjusting the solution pH value and then make the physicochemical properties of the drug-loaded micelles change; namely, they are stable in normal physiological conditions and dissociate in acidic environments, thus achieving the fixed-point release of drugs [26]. Poly(2-(dimethylamino)ethyl methacrylate (PDMAEMA) is a pH-sensitive polymer that has good antibacterial properties and molecular weight-dependent cytotoxicity [27,28]. The degree of protonation of DMAEMA's tertiary amines is different under different pH conditions, resulting in a change in the hydrophilic/hydrophobic equilibrium of the polymer chain segments with a change in the pH. It was reported that the dissociation constant (pKa) of PDMAEMA is approximately 7.1-7.3 [27,29-31]. When the pH value is less than the pKa, the protonation ability of tertiary amine groups is enhanced, and the solubility of polymers in aqueous solution is increased, thus showing hydrophilicity. In contrast, when the pH value is greater than the pKa, the deprotonation of tertiary amines is enhanced, and the solubility is decreased, thus showing hydrophobicity. Zhou et al reported a dual pH-sensitive supramolecular star polymer that has a strong inhibitory effect on the proliferation of tumor cells [32].

Although the host-guest interaction between β-CD and azobenzene has been extensively studied, most of the drug carriers are focused on single stimulus-responsive supramolecular polymers [14,18-21,23]. This class of single stimulus-responsive supramolecular polymers generally has relatively low release accuracy and exhibits some side effects; in particular, they cannot sufficiently respond to complex microenvironment changes in cancer cells in that the change in the behavior of cancer cells is more often a result of a combinational change in multiple stimuli rather than that

of a single stimulus [24]. Since dual and/or multiple stimuli responsive supramolecular polymers can provide a unique opportunity to fine-tune their response to each stimulus independently, to expand the controlled release modes and comprehensively modulate drug release profiles *via* the synergistic response to different stimuli [15], it is highly necessary to design and develop dual- and/or multi-stimuli responsive supramolecular drug-loaded micelles. Especially, the synergistic effect between these different stimuli responsive components is expected to offer more efficient targeted release in cancer microenvironments in comparison to a single stimulation but maintain better stability in normal cells and reduce the damage to healthy tissues, thus maximizing the functions of the supramolecular polymers.

Against this background, our objective is to construct a supramolecular polymer, β-CD-*graft*-PDMAEMA@Azo modified poly(ε-caprolactone) (β-CD-*g*-PDMAEMA@Azo-PCL), through the host-guest inclusion complexation interactions between β-CDs and Azo groups; the host polymer β-CD-*g*-PDMAEMA and a guest polymer Azo-PCL were synthesized through atom transfer radical polymerization (ATRP) and ring opening polymerization (ROP), respectively. Herein, hydrophobic PCL constitutes the core of supramolecular micelles, and hydrophilic PDMAEMA is used as the shell of supramolecular micelles for sensing pH changes. Azobenzene is a typical photoresponsive group, which is used to sense the change in light conditions. The drug loading behavior of supramolecular polymer micelles and the effect of external environmental stimuli, such as light conditions and pH values, on the drug release rate are studied using DOX as a hydrophobic drug model. We expect that the developed supramolecular polymer micelles can accomplish more precise drug release in cancer microenvironments and maximize the release amount of drugs at lesion or cancer

locations through the synergistic response to multiple stimuli, thus achieving optimal bioavailability and targeting efficiency of drugs.

2. Experimental section

2.1 Materials and reagents

Beta-cyclodextrin (β-CD, 99%) and 6-chlorohexanol (CH, 98%) were purchased from the Saan Chemical Technology (Shanghai) Co., Ltd., China, and β-CD was dried in vacuum at 100 °C for 24 h before use. 2-Bromoisobutyryl bromide (BIBB, 98%), tris(2-(dimethylamino) ethyl) amine (Me_6TREN, >98%), cuprous bromide (CuBr, 98%) and N,N-(dimethylamino)ethyl methacrylate (DMAEMA, 99%) were obtained from the Aladdin Industrial Corp., Shanghai, China. CuBr was treated before use by the following method: CuBr was first stirred in glacial acetic acid until it became white and then filtered. The solid was washed with ethyl alcohol three times, then washed with diethyl ether two times and finally dried in vacuum at 80 °C for 2 h. 4-(Phenyldiazenyl)phenol or 4-(phenylazo)phenol (Azo, 98%) and ε-caprolactone (ε-CL, 99%) were supplied by the Macklin Biochemical Co., Ltd., Shanghai, China, and used as received. Stannous octoate ($Sn(Oct)_2$), potassium iodide (KI), potassium carbonate (K_2CO_3), chloroform ($CHCl_3$), dichloromethane (CH_2Cl_2), acetone and anhydrous ether were provided by the Sinopharm Chemical Reagent Co., Ltd., Shanghai, China, and used directly. Magnesium sulfate ($MgSO_4$) was supplied by the Tianjin Kemio Chemical Reagent Co., Ltd., Tianjin, China. N,N-Dimethylformamide (DMF), methanol (CH_3OH), ethyl alcohol (C_2H_5OH), ethyl acetate (EA), petroleum ether (PE), and triethylamine (TEA, 99%) were obtained from the Tianjin Fuyu Fine Chemical Co. Ltd., Tianjin, China. DMF was distilled before use to remove moisture. Doxorubicin hydrochloride

(DOX·HCl, 98%) were afforded by the Macklin Biochemical Co., Ltd., Shanghai, China, and used as received.

2.2 Experimental procedure

Preparation of the supramolecular polymer β-CD-g-PDMAEMA@Azo-PCL was achieved through a three-step process, which includes synthesis of a host polymer β-CD-g-PDMAEMA, a guest polymer Azo-PCL and a supramolecular polymer

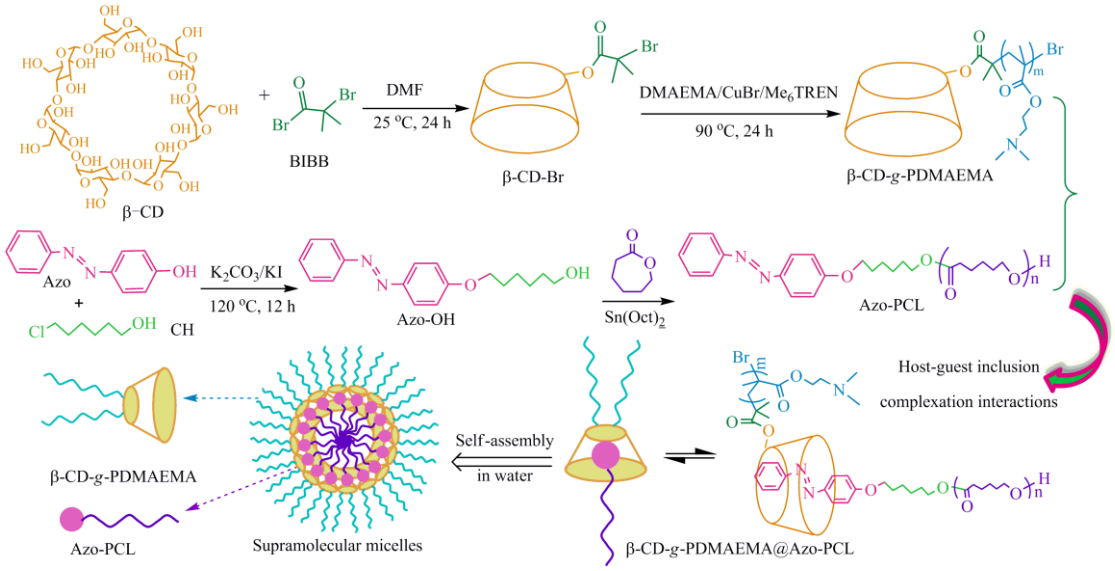

Scheme 1 Preparation strategy sketch map of β-CD-*g*-PDMAEMA@Azo-PCL supramolecular polymers and their self-assembled micelles.

β-CD-g-PDMAEMA@Azo-PCL, as shown in Scheme 1.

2.2.1 Synthesis of bromide modified β-CD initiator (β-CD-Br)

The synthesis of bromide modified β-CD initiator, β-cyclodextrin acyl bromide (β-CD-Br), was attained through an acyl bromide reaction of β-CD and BIBB in a molar ratio of β-CD to BIBB of 1:4. In detail, 5 g (4.4 mmol) of β-CD (^{1}H NMR and ^{13}C NMR spectra are shown in Figure S1 of the Supporting information (SI)) was dissolved in 34 mL of anhydrous DMF in a 100 mL Schlenk flask with stirring, and then, it was

cooled to 0 °C in an ice bath. An aliquot of 2.175 mL (17.6 mmol) of BIBB was dissolved in 6 mL of anhydrous DMF, and then, the solution was added dropwise to the β-CD solution with a syringe under a N_2 atmosphere. The reaction mixture was stirred at 0 °C for 2 h and then at 25 °C for 24 h. The final reaction mixture was precipitated with an excess of anhydrous diethyl ether and centrifuged. The crude product was washed with acetone three times and then dried in a vacuum desiccator overnight at 35 °C, giving a purified white solid product β-CD-Br (*Mean yield*: 60%). ^{1}H NMR (400 MHz, DMSO-d_6, δ in ppm): 4.79 (s, 7H), 4.16-4.40 (s, 7H), 3.50-3.82 (m, 28H), 3.27–3.32 (m, 14H), 2.04 (s, 12H); ^{13}C NMR (400 MHz, DMSO-d_6, δ in ppm): 162.8, 102.37, 81.96, 73.50, 72.84, 72.47, 60.35, 56.49, and 34.73. The ^{1}H NMR and ^{13}C NMR spectra are shown in Figure S2 (SI).

2.2.2 Preparation of the host polymer β-CD-*g*-PDMAEMA

β-CD-graft-poly(2-(dimethylamino)ethyl methacrylate) (β-CD-*g*-PDMAEMA) was synthesized by the ATRP of DMAEMA using β-CD-Br as an initiator and CuBr/Me_6TREN as a catalytic system in a molar ratio of β-CD-Br/DMAEMA/Me_6-TREN/CuBr =1:120:3:2. In a typical experiment, β-CD-Br (0.2149 g, 0.15 mmol), 6 mL of anhydrous DMF and DMAEMA (3.033 mL, 18 mmol) were successively added into a 50 mL dried Schlenk flask. The mixed solution was degassed by a freezing–pumping–thawing process to remove oxygen and moisture, followed by suffusing with a N_2 atmosphere. Me_6TREN (120 μl, 0.45 mmol) was added fleetly into the reaction flask under the N_2 atmosphere, and then, an immediate freeze–pump–thaw operation was conducted. Then, CuBr (43 mg, 0.3 mmol) was swiftly added into the flask under N_2 flow by repeating the above operation. The reaction flask was sealed, and the polymerization reaction was carried out at 90 °C for

12 h under magnetic stirring. After the reaction was completed, the final mixture was diluted with THF and passed through a short neutral alumina column to remove the copper catalyst. The solvent was then removed by rotary evaporation, and the residual solution was transferred to a dialysis bag with a MWCO of 2000 to dialyze against 500 mL deionized water for 48 h to remove residual monomers. The dialysate was collected and lyophilized to give 0.74 g (*Mean yield*: 24.3%) of white solid β-CD-*g*-PDMAEMA, and the monomer conversion was estimated to be approximately 18.6% based on a gravimetric method and 27.5% by ^{1}H NMR. Thus, the theoretical and experimental molecular weights were approximately 4940 and 6620 g mol^{-1}, respectively. ^{1}H NMR (400 MHz, $CDCl_3$, δ in ppm): 4.04 (t, J=3.6 Hz, 66H), 2.55 (t, J=6.4 Hz, 66H), 2.27 (s, 198H), 1.80-1.89 (m, 66H), 0.89-1.13 (m, 99H), 5.00 (s, 7H), 3.57 (m, 28H), 3.43 (m, 14H), and 2.11 (s, 12H); ^{13}C NMR (400 MHz, $CDCl_3$, δ in ppm): 177.42, 176.73, 63.14, 57.13, 54.15, 45.92, 44.73, 29.80, 18.64, and 16.74 [33]; $M_{n,LLS-GC}$=12900 g mol^{-1} and PDI=1.39. The ^{1}H NMR and ^{13}C NMR spectra are shown in Figure S3 (SI).

2.2.3 Preparation of 6-(4-(phenyldiazenyl)phenoxy)hexan-1-ol (Azo-OH)

Azo-OH was prepared by the Williamson etherification reaction of 4-(phenyldiazenyl)phenol and 6-chlorohexanol. 4-(Phenyldiazenyl)phenol (4.9565 g, 25.0 mmol), 6-chlorohexanol (5 mL, 37.5 mmol), K_2CO_3 (5.1815 g, 37.5 mmol), and KI (0.0415 g, 0.25 mmol) were solubilized in 100 mL of dried DMF in a 250 mL round-bottom flask to obtain a mixed solution. The mixed solution was refluxed at 120 °C for 12 h to afford a red-brown solution. The resulting solution was washed with a large amount of water to dissolve K_2CO_3, and then, the resultant solution was repeatedly extracted three times using chloroform to remove K_2CO_3. The solution was re-extracted with deionized water thrice to remove DMF. The product was dried with anhydrous

$MgSO_4$ and filtered; the filtrate was evaporated by rotatory evaporation to remove most of the solvent. The concentrate was purified by column chromatography using silica gel as a stationary phase and petroleum ether and ethyl acetate (*v/v*=6:1) as an eluent. An orange flake crystal product was obtained by rotary evaporation and then dried in vacuum at 35 °C for 24 h (*Mean yield*: 77%). ^{1}H NMR (400 MHz, $CDCl_3$, δ in ppm): 7.95–7.81 (m, 4H), 7.55–7.38 (m, 3H), 7.04–6.94 (m, 2H), 4.04 (t, *J*=6.5 Hz, 2H), 3.66 (t, *J*=6.5 Hz, 2H), 1.83 (dq, *J*=8.1, 6.5 Hz, 2H), 1.63–1.63 (m, 2H), 1.55–1.42 (m, 4H), 1.39 (s, 1H); ^{13}C NMR (400 MHz, $CDCl_3$, δ in ppm): 161.69, 152.78, 146.86, 130.39, 129.08, 124.81, 122.58, 114.72, 68.22, 62.76, 32.65, 29.19, 25.89, and 25.58. The ^{1}H NMR spectrum with integrals and ^{13}C NMR spectrum are incorporated in Figure S4 (SI), showing that Azo-OH was sufficiently purified.

2.2.4 Preparation of the guest polymer Azo-PCL

Azobenzene initiated polycaprolactone (Azo-PCL) as a guest polymer was prepared by ROP of ε-CL using Azo-OH as an initiator. Representatively, Azo-OH (0.200 g, 0.67 mmol), ε-CL (2.975 mL, 26.85 mmol), and a catalytic amount of $Sn(Oct)_2$ (0.033 mL, 0.10 mmol) were quickly added into a 50 mL dried Schlenk flask. The system was degassed by a freeze–pump–thaw operation repeated three times to eliminate oxygen and ultimately suffused with nitrogen gas. The mixture was heated to 120 °C to start the polymerization with persistent stirring. After 24 h, the reactor was exposed to air to terminate the reaction, offering a brownish red viscous liquid. The resulting solution was diluted with CH_2Cl_2, precipitated into an excess of cold methanol twice, and centrifuged. The resultant product was dried in a vacuum desiccator at 35 °C overnight, giving a yellow solid, which was named Azo-PCL (*Mean yield*: 85%). ^{1}H NMR (400 MHz, $CDCl_3$, δ in ppm): 7.86 (m, 4H), 7.45 (m, 3H), 6.97 (m, 2H), 4.06 (t, *J*=6.7 Hz, 130H),

3.63 (t, *J*=5.6 Hz, 4H), 2.30 (t, *J*=7.5 Hz, 128H), 1.80 (m, 2H), 1.61 (m, 256H), 1.38 (m, 132H); ^{13}C NMR (400 MHz, $CDCl_3$, δ in ppm): 173.50, 161.56, 152.71, 146.62, 130.29, 128.98, 124.70, 122.49, 114.63, 68.06, 64.10, 63.62, 34.08, 32.29, 28.54, 28.30, 25.69, 25.49, 25.29, and 24.54; $M_{n,NMR}$=7700 g mol^{-1}, $M_{n,LLS-GC}$=8000 g mol^{-1} and PDI=1.20. The ^{1}H NMR and ^{13}C NMR spectra are incorporated in Figure S5 (SI).

2.2.5 Preparation of the supramolecular micelles

β-CD-*g*-PDMAEMA@Azo-PCL supramolecular assemblies were prepared by a host-guest inclusion complexation interaction between β-CD and azobenzene at molar ratios of β-CD-*g*-PDMAEMA:Azo-PCL of 0.5:1, 1:1 and 1.5:1 through a dialysis technique, as illustrated in Scheme 1. Briefly, 15 mg of β-CD-*g*-PDMAEMA and 28.9 mg (3.75×10^{-3} mmol) of Azo-PCL were separately dissolved in DMF to form a 5 mg mL^{-1} solution and stirred for 30 min. Then, the Azo-PCL solution was added dropwise to the β-CD-*g*-PDMAEMA solution and stirred for 30 min. Deionized water (2 mL) was added dropwise into the mixed solution at a rate of 5 μl s^{-1} under vigorous stirring until the solution became turbid to induce the formation of supramolecular micellar assemblies. After the stirring was performed for 4 h, the β-CD-*g*-PDMAEMA@Azo-PCL solution was transferred into a dialysis bag (MWCO: 2000) for dialysis at room temperature for 48 h to completely remove DMF. Fresh deionized water was replaced hourly for the first 3 h and then once every 6 h. A fraction of the dialysate was collected and lyophilized for 24 h, affording cream-colored or beige supramolecular polymer β-CD-*g*-PDMAEMA@Azo-PCL; another part of the dialysate was collected in a 50 mL volumetric flask for further measurements. ^{1}H NMR (400 MHz, $CDCl_3$, δ in ppm): 6.94-7.82 (m, 9H), 3.99 (t, J=5.6 Hz, 196H), 3.60 (t, *J*=6.7 Hz, 4H), 2.51 (t, J=6.7 Hz, 66H), 2.23 (m, 326H), 1.76 (m, 66H), 1.59 (m, 256H), 1.32 (m,

134H), and 0.82-0.98 (m, 99H); ^{13}C NMR (400 MHz, $CDCl_3$, δ ppm): 177.43, 173.73, 64.27, 63.14, 57.13, 54.11, 45.91, 44.74, 34.21, 29.81, 28.43, 25.61, 24.67, 18.60, and 16.64. The details are described in Figure 1.

2.3 Measurements and characterization

^{1}H nuclear magnetic resonance (NMR) and two-dimensional nuclear Overhauser effect spectroscopy of NMR (2D NOESY ^{1}H NMR) analyses were performed on a 400 MHz JNM-ECZ400S/L1 spectrometer (JEOL Corp., Japan) using $CDCl_3$ or DMSO-d_6 as the solvent and tetramethylsilane (TMS) as the internal standard substance. Fourier transform infrared spectra (FT-IR) were recorded on a Tensor II Fourier transformation infrared spectrophotometer (Bruker Corp., Germany), and samples were pressed into KBr pellets. A laser light scattering gel chromatography system (LLS-GC, VISCOTEK TM, Marvin Corp., UK) was used to determine the number-averaged molecular weight (M_n) and polydispersity index ($PDI=M_w/M_n$). The calibration was conducted by using polystyrene (PS) standards, and the refractive index increment (dn/dc) values of the PS, host and guest samples were determined to be 0.185, 0.181 and 0.087 mL g^{-1}, respectively, at 35 °C using chromatography grade THF containing 2.5% TEA as the mobile phase. Before measurement, the dried polymers were dissolved in THF/TEA to form a concentration of 2 mg mL^{-1}. The polymer solutions were filtered through a 0.22 μm needle-type Teflon filter (organic, Φ13 mm). The measurement was performed at a flow rate of 1.0 mL min^{-1} at a column temperature of 35 °C.

The fluorescence spectra were recorded on a fluorescence spectrophotometer (FluoroMax-4, HORIBA Scientific, Japan) using pyrene as a probe to measure the critical micelle concentration (CMC). In detail, 5.0565 mg of pyrene was accurately weighed, dissolved in acetone, and brought to volume in a 50 mL brown volumetric

flask, offering a pyrene solution concentration of 5×10^{-4} mol L^{-1}. The pyrene solution (6 μl) was placed into a 10 mL sample tube, and the acetone was completely evaporated in an oven. Then, 5 mL of micelle solution with a concentration (C) of 1×10^{-4}~5×10^{-1} mol L^{-1} was added to the sample tube containing pyrene and magnetically stirred for 12 h for fluorescence spectrum scanning. The excitation wavelength was set as 330 nm, the wavelength range was from 350 to 550 nm, and the slit width was 1 nm. The CMC values were obtained by calculating the fluorescence intensity ratio (I_3/I_1) at 384 nm (I_3) and 373 nm (I_1) from the emission spectra, plotting the I_3/I_1-logC curves, and determining the concentration corresponding to the intersection of the two tangents.

The ultraviolet–visible (UV–vis) absorption spectra were recorded on a UV-6100S UV–vis spectrophotometer (Maipuda Instrument Co., Ltd., Shanghai, China) to measure the light responsiveness and loading ability for the drug of the prepared supramolecular polymer assemblies and to monitor the absorbance and drug release behavior of DOX-loaded supramolecular assemblies. A UV-light irradiator (365 nm, 6 W, ZF-5 Lamp) and a visible-light irradiator (450 nm, 3 W, POLICE) were used to induce the photoisomerization of Azo-PCL and the supramolecular assembly containing Azo moieties, with a radiation distance of 5 cm. The morphologies and sizes of the supramolecular assemblies before and after DOX was loaded were observed on an ultrahigh-resolution JEM-2100 TEM (JEOL Corp., Japan) at an accelerating voltage of 200 kV. The samples were prepared by placing two drops of the micelle solutions on the copper grid with carbon films and dried at room temperature. A laser particle analyzer and dynamic light scattering device (DLS, BI-90Plus, Brookhaven, USA) equipped with a 15 mV argon ion laser operating at a scattering angle of λ=660 nm were used to measure the hydrodynamic diameter (D_h) and particle size distribution (PDI) of

the assemblies at a sample concentration of 0.5 mg mL^{-1}. The measurements were carried out at a deflection angle of 90° and output power of 15 mW at room temperature.

2.4 Loading and *in vitro* controlled release of the drug

Twenty milligrams (0.0345 mmol) of DOX·HCl was dissolved in 6 mL of DMF, followed by 15 μl (0.1079 mmol) of TEA to remove HCl, and the solution was stirred in the dark environment at room temperature for 4 h. Sixty milligrams of β-CD-*g*-PDMAEMA@Azo-PCL supramolecular assemblies was then dissolved in DMF/H_2O (7.2 mL, *v/v*=1:2) with vigorous stirring for 2 h to ensure sufficient inclusion complexation. The DOX solution was added dropwise to the above inclusion complex solution without light under stirring for 6 h. Then, 3 mL of deionized water was added into the mixture at a rate of 5 μl s^{-1} under rapid stirring until the solution became turbid, indicating the formation of the micellar solution, and it was kept stirring away from light overnight. After that, the solution was dialyzed (MWCO: 2000) against 800 mL of deionized water for 24 h to remove free DOX and DMF. Fresh deionized water was replaced approximately every 4 h, giving the resultant DOX-loaded β-CD-*g*-PDMAEMA@Azo-PCL micelle nanoparticles, denominated as DOX-β-CD-*g*-PDMAEMA@Azo-PCL. The DOX-loaded nanoparticles were collected and freeze-dried for further measurements, affording a brownish red solid. To quantify the loading capacity (LC) and entrapment efficiency (EE), 4 mg of the lyophilized DOX-loaded nanoparticles were dissolved in 200 mL of DMF. A UV-visible spectrophotometer (UV-6100S, Maipuda, Shanghai, China) was used to monitor the absorbance of the solution at 490 nm, and the LC and EE were calculated according to Formulas (1) and (2), respectively:

LC(%)=(Mass of DOX in nanoparticles/Mass of DOX-loaded nanoparticles)100% (1)

EE(%)=(Mass of DOX-loaded in nanoparticles/Mass of DOX in feed)100% (2)

Prior to measurements, calibration was performed with DOX standard solution in DMF at 490 nm. The calibration equation with a high squared correlation coefficient of R^2=0.9995 was obtained as follows:

$C\ (mg\ mL^{-1})=(A+0.0150)/18.7583$ (3)

where C is the concentration of DOX in the solution and A is the absorbance at 490 nm. The LC and EE values were determined to be approximately 13.2 and 66.1 %, respectively.

To demonstrate the pH and light responsive release behavior, 4 mg of lyophilized DOX-loaded supramolecular polymer was dispersed in 4 mL of phosphate buffered saline (PBS) with a pH of 7.4, 6.0 or 5.0 to offer a concentration of 1 mg mL^{-1}, and then, it was dialyzed (MWCO: 3500) in 200 mL of the above PBS at 37 °C with or without UV-irradiation (365 nm, 8 W, ZF-7A lamp). At a given time interval, aliquots of 4 mL were withdrawn from the beaker to measure the amount of DOX released in the dialysate using a UV-vis spectrophotometer at a λex of 490 nm and replaced with an equal volume of fresh PBS. The cumulative DOX release was estimated based on the calibration curves of DOX in PBS (R^2=0.9999) according to the following equation:

$M_t=(A+8.6647\times10^{-4})/6.8117$ (4)

Cumulative DOX release (%)=$M_t/M_0\times100\%$ (5)

where M_t represents the amount of DOX released at time t and M_0 is the amount of DOX loaded in the β-CD-*g*-PDMAEMA@Azo-PCL micelle nanoparticles.

2.5 MTT assay

The cytotoxicities of free DOX, the blank and DOX-loaded supramolecular micelles

toward HeLa cells were evaluated by the 3-(4,5)-dimethylthiahiazo(-z-y1)-3,5-diphenytetrazoliumromide (MTT) assay. HeLa cells were seeded in a 96-well plate at a density of 1×10^4 per well and cultured in a DMEM medium supplemented with 10 % (*v/v*) fetal bovine serum (FBS), 0.1 % penicillin-streptomycin and 5 % CO_2 at 37 °C for 24 h. After that, the HeLa cells were cultured in 200 μl of fresh DMEM medium containing the above samples and further incubated for another 24 h. The cells were eluted with PBS thrice to remove the metabolites, and the growth of cells ceased. Afterwards, the medium was substituted with 200 μl of fresh DMEM containing 20 μl of 5 mg mL^{-1} sterile filtered MTT and incubated for additional 4 h. Then, the supernatant was discarded, the purple formazan crystals generated by live cells were dissolved in 150 μl of DMSO, and shaking was performed for 10 min. At the same time, HeLa cells were planted in DMEM and reproduced under the same conditions as a control group. The absorbance of the solution was recorded by a universal microplate reader (Bio-Rad Laboratories (UK) Ltd) at 570 nm, and the cell viability was calculated as follows:

$$\text{Cell viability (\%)} = (OD_{sample}/OD_{control})100\% \quad (6)$$

where $OD_{control}$ and OD_{sample} are the optical densities of the sample and control group, respectively. The student's t-test was used to determine the significance of any pairs of observed differences. Differences were considered to be statistically significant at $p<0.05$. The results were averaged from the data of five measurements and expressed as the mean value±SD.

3. Results and discussion

3.1 Structural characterization

Figures 1(A) and 1(B) depict the ^{1}H and ^{13}C NMR spectra of β-CD-*g*-PDMAEMA@Azo-PCL, respectively, and the ^{1}H NMR and ^{13}C NMR spectra of their precursors, host polymer β-CD-*g*-PDMAEMA and guest polymer Azo-PCL are shown in Figures S1-S5 (SI). Figures S1 and S2 (SI) manifest the successful preparation of β-CD-Br, and two –OH groups in the whole β-CD structure are proven to participate in the reaction by calculating the integration area ratio (A) of the peak at 4.79 ppm to the peak at 2.04 ppm (A is approximately 1:1.67, and n=7×1.67/6≈2). The host polymer β-CD-*g*-PDMAEMA is synthesized *via* ATRP, as shown in Figure S3 (SI), and the degree of polymerization for PDMAEMA is estimated to be approximately 33 by comparing the integration area ratio of the -$(CH_3)_2$ peak in BIBB at 2.11 ppm to the -CH_2- peak in PDMAEMA at 4.04 ppm. Hence, the experimental number-averaged molecular weight ($M_{n,NMR}$) of β-CD-*g*-PDMAEMA is approximately 6620 g mol^{-1}. The syntheses of the guest polymer Azo-PCL and its precursor are magnified by Figures S4 and S5 (SI). The degree of polymerization for PCL is estimated to be approximately 65 by comparing the integration area ratio of the peak at 6.95-7.01 ppm to the peak at 2.29 ppm, offering the experimental number-averaged molecular weight ($M_{n,NMR}$) of Azo-PCL of approximately 7,700 g mol^{-1}. In ^{1}H and ^{13}C NMR spectra of the supramolecular polymer β-CD-*g*-PDMAEMA@Azo-PCL in Figures 1(A) and 1(B), it can clearly be observed that all of the characteristic proton and carbon shift signals attributed to the host polymer β-CD-*g*-PDMAEMA and the guest polymer Azo-PCL can be observed, of which the peaks in the ^{1}H NMR spectrum at 3.99 and 2.23 ppm are overlapped; they are ascribed to the methylene protons attached to the -CH_2-$\underline{CH_2}$-OCO- structure and the methyl and methylene protons in the -N$\underline{(CH_3)_2}$/-CH_2-$\underline{CH_2}$-CO- structure in the host and guest polymers, indicating that the

β-CD-*g*-PDMAEMA@Azo-PCL supramolecular polymer is successfully assembled by

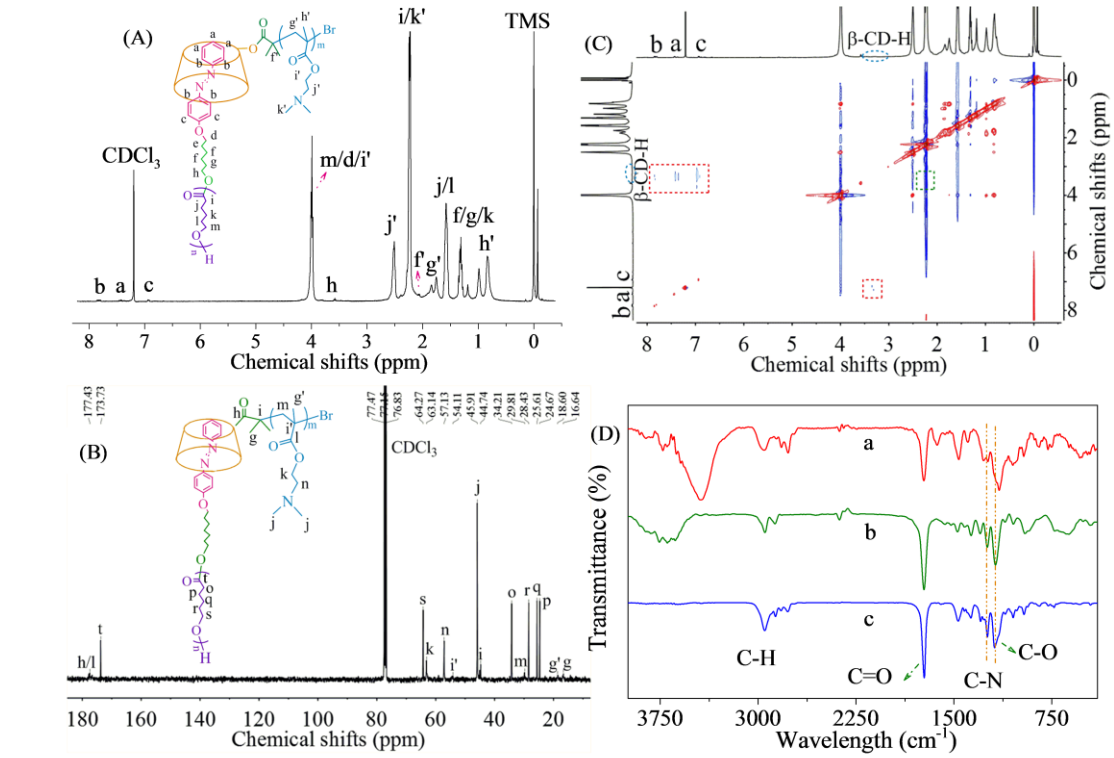

Figure 1 (A) ^{1}H NMR, (B) ^{13}C NMR and (C) 2D NOESY ^{1}H NMR spectra of β-CD-*g*-PDMAEMA@Azo-PCL supramolecular micelles/assemblies with [host]/[guest]=1:1 in $CDCl_3$, and (D) FT-IR spectra of (a) β-CD-*g*-PDMAEMA, (b) Azo-PCL and (c) β-CD-*g*-PDMAEMA@Azo-PCL.

the aid of the host–guest inclusion complexation between β-CD and Azo groups [33].

The host–guest inclusion complexation between β-CD and Azo groups is proven by 2D NOESY ^{1}H NMR, as shown in Figure 1(C). Clearly, the proton signals of β-CD at 3.30-3.55 ppm are associated with those of the azo protons at 6.94-7.82 ppm, giving some cross-peaks (red circles in Figure 1(C)); this suggests that β-CD can interact with azobenzene moieties to form a host-guest inclusion complexation system, and the azobenzene-containing PCL moieties are entrapped in the cavity of β-CD [8,14,22,34,35]. On the other hand, the possibility of the intermolecular and/or

intramolecular host–guest interactions between β-CD and PDMAEMA moieties cannot be excluded because the hydrophobic effect of PDMAEMA may exist when the pH>pKa due to the weakened protonation, thus leading to a fast decrease of the hydrophilicity. It can be seen from the green circle in Figure 1(C) that the proton signals of β-CD at 3.30-3.55 ppm are correlated with those of dimethylamino(ethyl) groups of PDMAEMA moieties at approximately 2.25 ppm, implying that β-CD can form supramolecular assemblies by complexing with side dimethylamino(ethyl) groups of PDMAEMA [36,37]. Therefore, it is confirmed that β-CD can interact not only with the azobenzene moieties but also with dimethylamino(ethyl) groups of PDMAEMA to form the host-guest supramolecular assemblies by inclusion complexation.

Figure 1(D) illustrates the FT-IR spectra of β-CD-*g*-PDMAEMA, Azo-PCL and β-CD-*g*-PDMAEMA@Azo-PCL. The host polymer β-CD-*g*-PDMAEMA produces the enhanced vibration peaks at 2930 and 2780 cm^{-1} as well as 1730 cm^{-1} ascribed to the C-H stretching and the C=O stretching, respectively, compared with its precursors β-CD and β-CD-Br shown in Figure S6(A) (SI). A new absorption peak emerges at 1238-1270 cm^{-1}, which is attributed to the C-N stretching in PDMAEMA chains. In the case of Azo-PCL, the –OH peak at 3305 cm^{-1} attributed to the –OH stretching of Azo-OH (Figure S6(B)) in associated and free states disappear. Meanwhile new absorption peaks emerge at 1728 and 1182 cm^{-1} separately attributed to the C=O and C-O-C stretching bands, manifesting the synthesis of the guest polymer through ROP. By comparing the FTIR spectra of β-CD-*g*-PDMAEMA and Azo-PCL with that of β-CD-*g*-PDMAEMA@Azo-PCL, it can be observed that the vibration peaks at 1728, 1243 and 1286 cm^{-1} reflecting the C=O, C-N and C-O stretching still exist, whereas the –OH stretching and the aromatic skeleton vibration bands are not observed, presumably

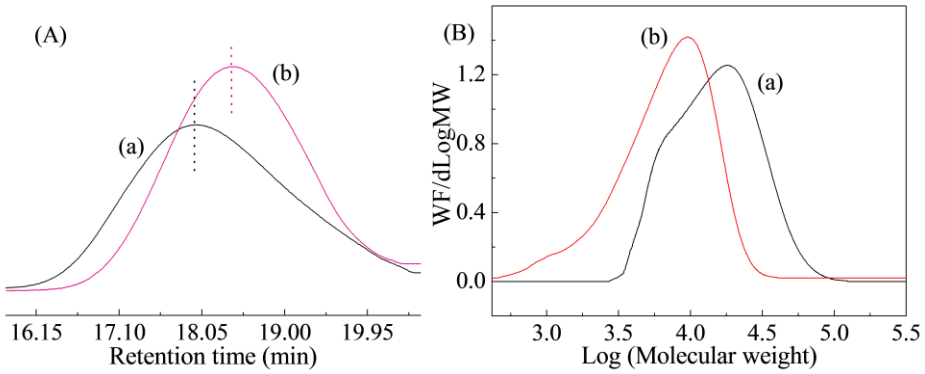

Figure 2 (A) LLS-GC traces and (B) the weight distribution curves of (a) β-CD-*g*-PDMAEMA and (b) Azo-PCL.

due to the inclusion of Azo-PCL in β-CD-*g*-PDMAEMA through the host-guest interactions. These findings indicate the preparation of β-CD-*g*-PDMAEMA@Azo-PCL. Figures 2(A) and 2(B) display the LLS-GC traces and the corresponding weight distribution curves of the host polymer β-CD-g-PDMAEMA and the guest polymer Azo-PCL. Their apparent Mn values are approximately 12,900 g mol^{-1} for β-CD-g-PDMAEMA and 8000 g mol^{-1} for Azo-PCL. The ^{1}H NMR Mn value, in particular, with respect to that of the host polymer, is lower than that by LLS-GC; this discrepancy is probably ascribed to the large hydrodynamic volumes of the host and guest polymer. However, it is higher than the estimated theoretical value based on a gravimetric method (4940 g mol^{-1}) due to the mass loss during preparation and post-treatment. Both of the traces present almost a symmetric unimodal distribution with almost no trailing. The LLS-GC weight distribution curves, however, demonstrate that the guest polymer Azo-PCL is nearly centrally distributed, giving a relatively low polydispersity index (PDI) of 1.20, whereas the host polymer β-CD-*g*-PDMAEMA generates a bump in the section of low molecular weight, leading to a slightly wider molecular weight distribution with a PDI of 1.39. In addition, the difference in the

number of –OH moieties involved in the reaction in each β-CD is responsible for the slightly higher PDI value, although there are, on average, two –OH groups in the entire β-CD structure participating in the reaction. Anyway, the experimental results indicate that the host and guest polymers are effectively purified and the polymerization processes are well controlled.

3.2 Self-assemblies and their physiochemical properties

The formation of the supramolecular assembly and the critical micelle concentration (CMC) were determined by a fluorescence spectrophotometer using pyrene as a fluorescent probe. The fluorescence intensity ratios (I_3/I_1) at 384 nm (I_3) and 373 nm (I_1) in the fluorescence emission spectra *vs*. the logarithm of the concentration (logC) was adopted to estimate the CMC value of the supramolecular self-assemblies, which is defined as the concentration corresponding to the intersection of the two tangents in I_3/I_1-logC curves [38], as tabulated in Table 1. It is clear that these supramolecular micelles possess CMC values below 111.9 mg L^{-1}, showing that they have good thermodynamic stability. As the molar ratio of the host polymer β-CD-*g*-PDMAEMA to the guest polymer Azo-PCL increases from 0.5:1 to 1.5:1, the CMC value of the

Table 1 CMC and DLS data of the supramolecular assemblies with various compositions and pH.

[Host]/[guest]	CMC (mg L^{-1})	D_h [a] (nm)	PDI	pH[b]	D_h [a] (nm)	PDI
0.5:1	111.9	213.6±20	0.121±0.008	3.4	310.4±44	0.405±0.030
1:1	68.4	272.0±42	0.211±0.020	7.4	222.3±30	0.319±0.040
1.5:1	52.6	286.0±60	0.249±0.053	8.0	290.5±25	0.197±0.017

[a] Concentration: 0.5 mg mL^{-1}, and [b] [host]/[[guest]=1:1

supramolecular self-assembly decreases from 111.9 to 52.6 mg L^{-1}. This finding is not consistent with the general theory that the greater the number of hydrophilic chain segments, the greater the CMC value of polymer micelles [38]. The reason for this phenomenon may be ascribed to the existence of hydrogen bonding interactions between the host polymer molecules, β-CD-g-PDMAEMA. With increasing the content of the host polymer, the hydrogen bond interactions are strengthened, whereas the (hydrogen bond) interactions between the supramolecular polymers and water molecules relatively decrease, leading to the decreased CMC values.

DLS is used to determine the hydrodynamic diameters (D_h) of the supramolecular polymer micelles and their distribution (*PDI*), and Table 1 summaries the DLS data of the prepared supramolecular self-assemblies with [host]/[guest] molar ratios of 0.5:1, 1:1 and 1.5:1. It can be found by comparing the three curves that the D_h values of the supramolecular self-assemblies increase from 213.6±20 nm to 286.0±60 nm as the proportion of the host polymer β-CD-g-PDMAEMA and the guest polymer Azo-PCL rises from 0.5:1 to 1.5:1; and they have a relatively low PDI value less than 0.25 but an increasing trend. The reason that for the increased D_h value with increasing content of the host polymer may mainly be related with the chain conformation of the PDMAEMA host polymers. Generally, during the formation of micelles, the Azo-PCL guest polymers, as hydrophobic fragments, construct the micellar cores, whilst the PDMAEMA host polymer chains, as hydrophilic segments, form the shells of the micelles, presenting an extended chain conformation. Consequently, the higher the proportion of the host polymer, the greater the content of the extended PDMAEMA chain segments, and thus, the larger the particle size of the supramolecular micelles.

Figure 3 displays TEM micro-images of the supramolecular self-assemblies having a

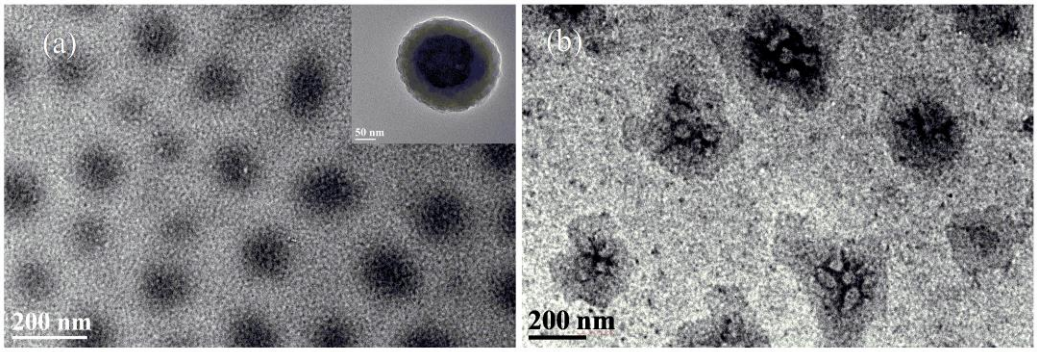

Figure 3 TEM microimages of the supramolecular self-assembly with [host]/[guest]=1:1 (0.5 mg mL^{-1}): (a) the original micelle and (b) the irradiated counterpart with 365 nm ultraviolet light. The inset in Figure 3(a) shows the TEM image of the DOX-loaded supramolecular micelle.

[host]/[guest] molar ratio of 1:1 at a concentration of 0.5 mg mL^{-1}. As shown in Figure 3(a), the supramolecular polymers spontaneously form a spherical core-shell micellar structure in aqueous solution through the host-guest inclusion complexation interactions, with the darker part in the center constituting the PCL core of the micelles and the lighter part in the periphery forming the PDMAEMA shell of the micelles. The self-assemblies have a uniform size distribution and an average diameter of ca. 167 nm. However, the particle size measured by DLS is generally much larger than that measured by TEM because the former offers hydrodynamic diameters in aqueous solution whereas the latter gives the particle size in a dried state. The extended or swelled micelles make the particle size of micelles increase significantly. In contrast, the drying process may be accompanied by the shrinkage of micelle particles, resulting in a smaller particle size.

3.3 Light and pH dual stimuli responsiveness

The supramolecular assembly containing azobenzene and tertiary amine groups is anticipated to exhibit photosensitive and pH sensitive responses. The light-responsive

feature can be proven by TEM images of the supramolecular assemblies ([host]/[guest]=1:1) after irradiation with 365 nm ultraviolet light, as illustrated in Figure 3(b). Clearly, one can observe that after UV irradiation, the regular spherical supramolecular micelles in Figure 3(a) change into irregular hierarchical assemblies and even some aggregates with various sizes, which is consistent with the results reported elsewhere [14,35,39,40]. The reason for this phenomenon is that the azobenzene units in the guest polymers are in a trans-configuration before UV light irradiation, which can enter the β-CD cavity through the host-guest interactions, self-assemble and form supramolecular micelles presenting spherical core-shell structures. Under ultraviolet light, azobenzene units undergo isomerization transformation from the trans- to cis-configuration, which does not match the cavity structure of β-CD. As a result, the Azo-PCL moieties depart from the cavity of β-CD, and the supramolecular assemblies dissociate into the host and guest parts. Considering the hydrophobicity of the cis-azobenzene-containing PCL chains and the hydrophilicity of PDMAEMA fragments, the wrecked host-guest system reconstructs new hydrophilic-hydrophobic balances, forming irregular hierarchical assemblies or aggregates with the hydrophobic Azo-PCL wrapped by the hydrophilic β-CD-*g*-PDMAEMA.

A UV-visible spectrophotometer is further used to investigate the light and pH responses of supramolecular polymer (micelle) solutions. Figure 4(a) shows the UV-vis spectra of a guest polymer, Azo-PCL, dissolved in DMF under UV light (365 nm) and visible light (450 nm) irradiation at different times. The characteristic absorption peaks at 350 and 440 nm are attributed to the π-π^* leap of trans-azobenzene and the n-π^* leap of cis-azobenzene, respectively [41]. Clearly, with the extension of the ultraviolet illumination time, the absorbance of Azo-PCL at 350 nm significantly decreases, while

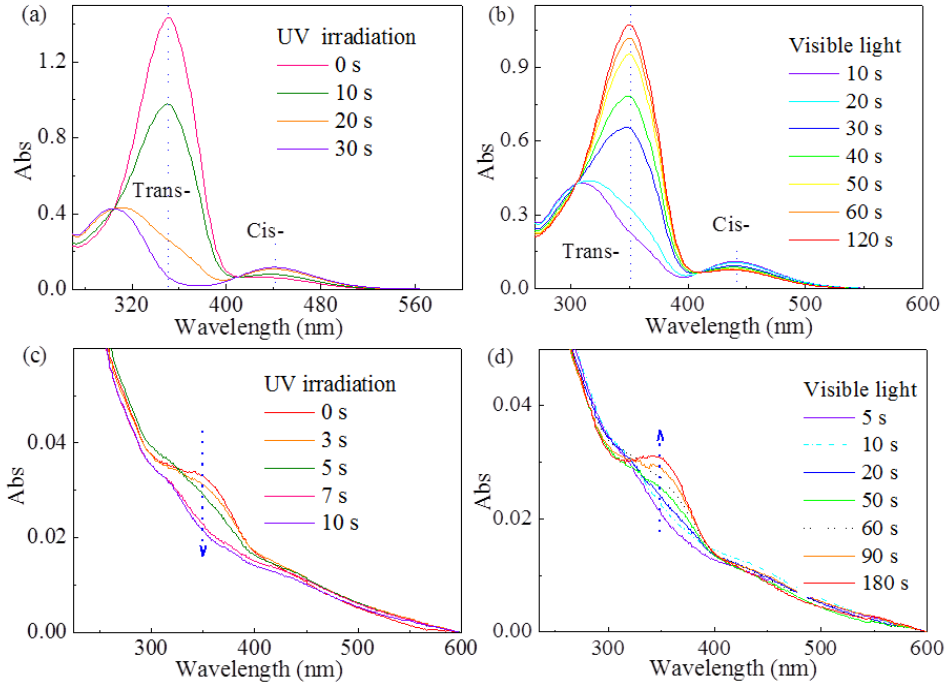

Figure 4 UV-vis spectra of (a and b) Azo-PCL (0.5 mg mL^{-1}) and (c and d) supramolecular self-assemblies (0.1 mg mL^{-1}, [host]/[guest]=1:1) under (a and c) 365 nm UV and (b and d) 450 nm visible irradiation.

the value at 440 nm slightly increases, indicating that azobenzene changes from the trans- to cis-configuration under ultraviolet irradiation. In contrast, with the extension of visible light time, the absorbance of Azo-PCL at 350 nm significantly increases, while the value at 440 nm slightly decreases, suggesting that azobenzene reversibly changes from the cis- to trans-configuration under visible light irradiation. Therefore, the supramolecular self-assemblies containing azobenzene units can reversibly self-assemble/dissociate by virtue of the trans→cis and cis→trans isomerization transition under alternating ultraviolet and visible light. On this basis, the absorption peak change at 350 nm was adopted to examine the trans→cis and cis→trans isomerization transition of the supramolecular assemblies with the [host]/[guest] ratio of 1:1, as depicted in Figures 4(c) and 4(d). With the extension of the ultraviolet irradiation

time, the absorbance of supramolecular micelles at approximately 350 nm decreases significantly, and the azobenzene units in the polymer change from the trans- to cis-configuration. With the extension of the visible light irradiation time, the absorbance of the supramolecular micelles at approximately 350 nm increases significantly, and the azobenzene units change from the cis- to trans-configuration. Under the alternating irradiation of ultraviolet and visible light, the cis-trans isomerization process of the azobenzene units can repeatedly be switched to a certain extent, signifying that the prepared β-CD-*g*-PDMAEMA@Azo-PCL polymer assembly has optical response performance.

Figure 5(a) shows the UV-vis transmittance of the prepared supramolecular assembly with a [host]/[guest] molar ratio of 1:1 at various pH values. Clearly, the supramolecular assembly micelles retain high transmittance in acidic solution below a pH of 4.8 and in alkaline environments above a pH of 8.0. The possibility is that in an acidic condition (pH=3-6), the protonation of tertiary amine groups in PDMAEMA side chains induces intermolecular and intramolecular electrostatic repulsion interactions between the amine groups, which avoids the aggregation among the supramolecular assemblies, resulting in the obviously increased light transmittance [42-44]. In addition, possible protonation of the azo groups in the azobenzene happens at different levels, and together with the electrostatic repulsion, it may cause disturbance to the host-guest inclusion complexation interaction of supramolecular micelles or/and produce tension on the hydrophobic cores, thus weakening but not wrecking the host-guest interaction between Azo and β-CD, which is in favor of the drug release [42,45]. It was reported that possible interactions of azobenzene with acidic groups would involve donation of the nitrogen lone pairs on the azo group to the Lewis acids or protonation of the nitrogen

[45]. This protonation of Azo-containing Azo-PCL is corroborated by UV-vis results, as shown in Figure S7 (SI). Clearly, the peak intensity at 350 nm at a pH of 3.4 is obviously lower than that at pH values 7.4 and 8.0 and aqueous solution due to probable protonation, and the peak position in various pH solutions is slightly red shifted to 358 nm compared with that in aqueous solution. Under alkaline conditions, the tertiary amine groups in PDMAEMA side chains undergo deprotonation, and then, the chain segments shrink. The shrunk PDMAEMA chains encase the host-guest system, which makes the size of the supramolecular micelles decrease compared with those in acidic and pH=7.4 solutions [27]. Even if the shrunk PDMAEMA chains may slightly aggregate into larger sizes during the experimental determination, the size is not enough

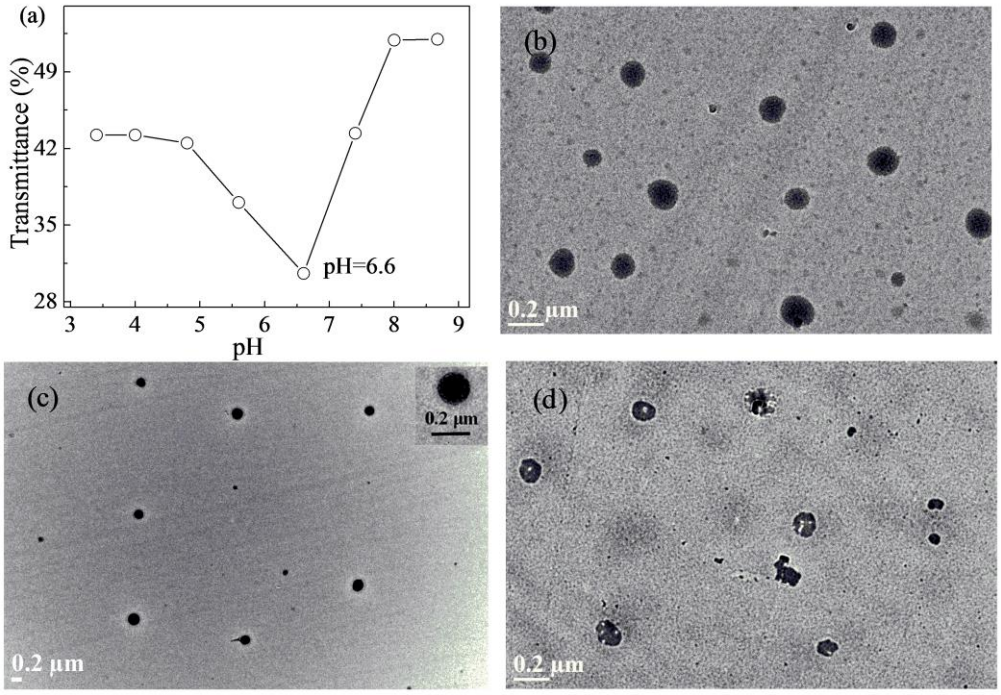

Figure 5 (a) UV-Vis transmittance change with pH for the supramolecular assembly with [host]/[guest]=1:1 and a concentration of 0.5 mg mL^{-1} and (b-d) TEM microimages of the supramolecular self-assemblies ([host]/[guest]=1:1; concentration: 0.5 mg mL^{-1}) in pH values of (b) 3.4, (c) 7.4 and (d) 8.0.

to cause the refraction and diffuse reflection of light, and it is not enough to induce precipitation, either. Therefore, the light transmittance increases significantly. Of course, with further extending the storage time, the shrunk polymers are gradually aggregated, and their size is gradually increased, finally leading to the production of precipitates. Thus, the solution becomes more transparent. It can further be observed from Figure 5(a) that when the pH is below 4.8, no obvious transmittance change is observed; as the pH of the solution increases from 4.8 to 6.6, the light transmittance decreases from 42.5 to 30.5% due to possible gradual deprotonation of the supramolecular assemblies. In contrast, when the pH is further elevated from 6.6 to 8.0, the tertiary amine groups in PDMAEMA chains are rapidly deprotonated, the PDMAEMA chains rapidly shrink, the size of the micelles decreases and the transmittance reaches up to 51.9%. The transmittance changes in different pH environments indicate that the β-CD-*g*-PDMAEMA@Azo-PCL supramolecular assemblies show obvious pH responsiveness.

The pH-induced responsiveness is further verified by DLS and TEM determination, as shown in Table 1 and Figure 5(b-d). It can be observed from Table 1 that the D_h values of the supramolecular self-assembly micelles first decrease and then increase when the pH value of the solution increases from 3.4 to 8.0. The reason for this phenomenon is that the tertiary amine groups of PDMAEMA segments possess a strong protonation capacity under acidic environments below the pKa, giving rise to an obviously increased electrostatic repulsion between the amine groups or PDMAEMA chains. This phenomenon leads to stronger hydrophilicity as well as large swelling of the micellar shells and offers a high D_h of 310.4 nm. Under normal physiological conditions close to the pKa of PDMAEMA, the PDMAEMA fragments collapse and shrink due to partial

deprotonation, producing a small D_h value of 222.3 nm. Hence, the synthesized supramolecular assemblies are relatively stable in normal physiological environments of the human body and suitable for blood circulation. Under alkaline environments, however, the tertiary amine groups undergo complete deprotonation, and the micelle particles tend to gather as the time prolongs, leading to the larger particle size of 290.3 nm than that at a pH of 7.4. Similar particle size changes are also proven by TEM analysis, as shown in Figure 5(b-d). When the pH is 3.4, the supramolecular micelles assume a nearly spherical core-shell micelle structure and have a slightly larger particle size of approximately 178 nm. This is because in an acidic medium at a pH of 3.4, the DMAEMA segments are protonated and hydrated, and the electrostatic repulsions between the amine groups are augmented, leading to swelling of the supramolecular assemblies and a large size, as mentioned above [46]. When the pH is increased up to 7.4, partial PDMAEMA chains are deprotonated, and the micelles retain a regular spherical morphology with a particle size of 167 nm as well as a good size distribution. When the pH reaches 8.0, PDMAEMA chains are almost completely deprotonated, and the PDMAEMA chains are shrunk; however, the shrunk chains still encase the host-guest system, forming smaller micelle assemblies. The size at a pH of 8.0 is approximately 120 nm, which is smaller than those at pH values of 3.4 and 7.4. This size is different from the DLS result, which demonstrated a larger size at a pH of 8.0 than at a pH of 7.4 because the measurements are conducted in different time intervals. At a pH of 8.0, with extension of the time, the deprotonated PDMAEMA segments may induce the coagulation of the micelles due to the increased hydrophobicity, and the size of the micelle nanoparticles is gradually increased. Due to the above possibility, the supramolecular assemblies show irregular morphologies and form small shrunk micelles

to slightly large aggregates at a pH of 8.0, as shown in Figure 5(d). These findings demonstrate the effect of the pH as a critical parameter to control the size and morphology of micelles, and they also prove the pH responsiveness of the supramolecular assemblies.

3.4 Loading and release of the drug from β-CD-*g*-PDMAEMA@Azo-PCL

The unique architecture and dual stimuli responsiveness for the supramolecular micelle self-assemblies is expected to greatly improve the LC and EE values as well as produce a synergistic target therapy against cancer cells. Given that the azo groups of the hydrophobic guest polymer Azo-PCL were included in the β-CD core of the host polymer β-CD-*g*-PDMAEMA, when the dialysis technique was used to prepare the drug-carrying micelles DOX-β-CD-g-PDMAEMA@Azo-PCL in aqueous solution, the DOX molecules without HCl were entrapped into the hydrophobic PCL inner core and the hydrophobic cavity of the azo-included β-CD portion, while the hydrophilic PDMAEMA fragments (pKa = 7.3) formed an outer layer, which supplied stability to the system. It is the β-CD hydrophobic cavity and the PCL hydrophobic core of the supramolecular polymer micelles that offer relatively high LC and EE values of approximately 13.2 and 66.1 %, respectively. The drug loading schematic diagram of DOX in the supramolecular self-assemblies is shown in Scheme 2. In fact, one can clearly observe from the inset in Figure 3(A) that the drug-loaded supramolecular micelles possess a significantly large particle diameter of approximately 256 nm, which is much larger than that of the blank micelles (167 nm); moreover, the kernel is noticeably darker. These findings further suggest that DOX has successfully entered into the hydrophobic core of PCL and the hydrophobic cavity of β-CD through hydrophobic interactions, forming the DOX-loaded supramolecular micelles, thus resulting in

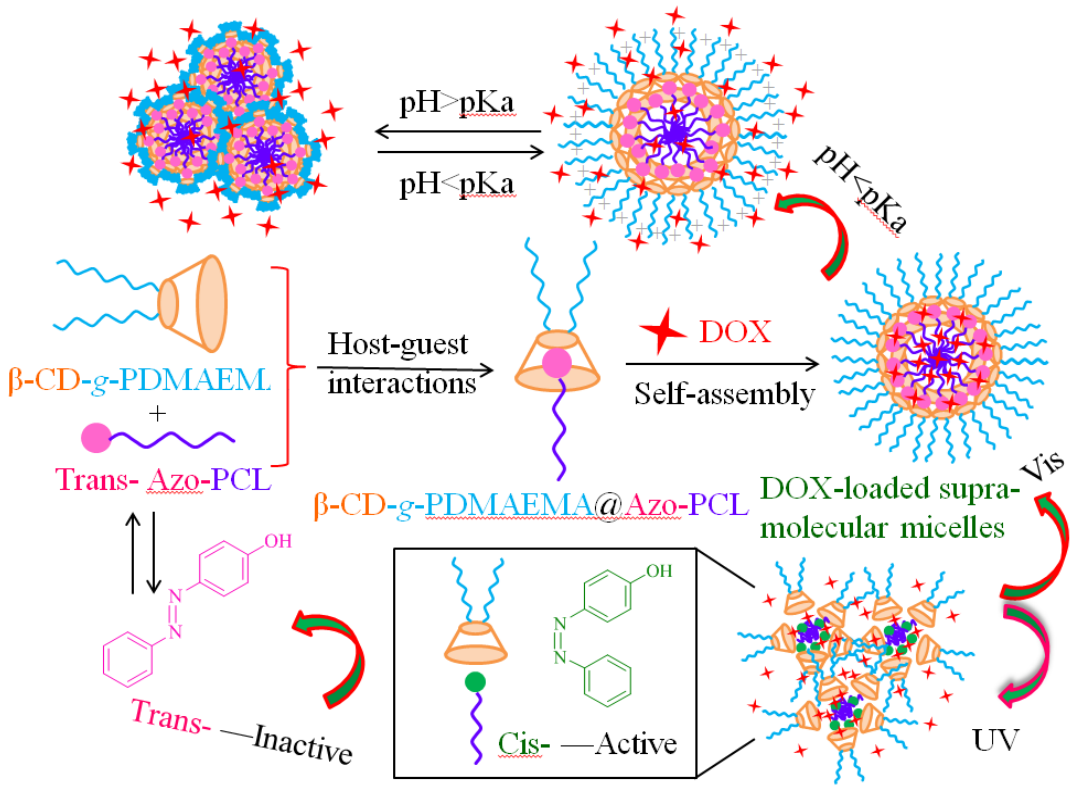

Scheme 2 Preparation and pH- and light-induced dual-stimuli-responsive drug release scheme of DOX-β-CD-*g*-PDMAEMA@Azo-PCL supramolecular self-assembly drug-loaded micelles.

volume expansion of the micelles.

To evaluate the effects of the light conditions and pH of the solution on the drug controlled release behavior, the DOX-β-CD-g-PDMAEMA@Azo-PCL drug-carrying micelles are dialyzed in the PBS solutions with pH values 5.0, 6.0 and 7.4 and/or different light conditions, giving the release profiles of DOX shown in Figure 6(A). It can be seen from Figure 6(A) that the DOX release amount was only approximately 26.2% after 30 hours of release when visible light irradiation is performed at 37 °C in a pH of 7.4. In contrast, the cumulative drug release is increased up to approximately 44.2% when the micelle solution is continuously irradiated with ultraviolet light, showing that the light condition has an obvious regulating effect on drug release. This is

because azobenzene is in the trans-configuration under visible light irradiation, which can enter into the β-CD cavity through the host-guest inclusion complexation interaction. The resulting supramolecular micelles are relatively stable, preventing the release of the drug from the inner core. Under ultraviolet light, the azobenzene changes from the trans- to cis-configuration, which does not match the β-CD structure. Hence, the supramolecular micelles dissociate, accelerating the release of the drug.

The relatively low DOX delivery amount of 26.2% in normal physiological environments (pH=7.4 and 37 °C) is attributed to the stable supramolecular micelles, as stated before. At this moment, the host-guest interaction between the β-CD and

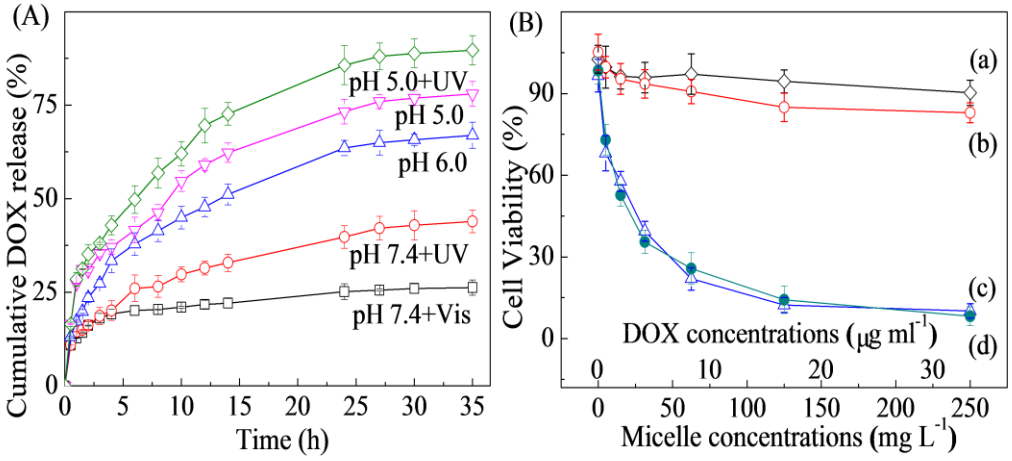

Figure 6 (A) Cumulative release of DOX from the supramolecular micelles in various pH environments under light conditions at a temperature of 37 °C and (B) cytotoxicity of a (a) blank supramolecular micelle, (b) DOX-loaded supramolecular micelle ([host]/[guest]=1:1) and (c) free DOX against HeLa cells incubated at 37 °C in PBS with a pH of 7.4 for 24 h as well as (d) DOX-loaded supramolecular micelles ([host]/[guest]=1:1) in PBS with a pH of 5.0 for 24 h and under UV irradiation for 10 s.

azobenzenes makes the resulting supramolecular micelles relatively stable, inhibiting the release of drug molecules to some extent. When the pH is below 7.3, the cumulative DOX release increases accordingly, and the release amount is enhanced with increasing the acidity from 67.0% at a pH of 6.0 up to 78.0% at a pH of 5.0 after 30 h of release, indicating that the pH value has a strong regulation effect on drug release. The possibility is that when the solution is acidic, the highly protonated PDMAEMA fragments bring about strong electrostatic repulsion interactions, thus triggering the passive release of DOX from the supramolecular assemblies [42]. The lower the pH (from 6.0 to 5.0) is, the higher the charge density on PDMAEMA chains is; this leads to more intensive electrostatic repulsion between hydrophilic PDMAEMA chains. Therefore, the chain segments are in a more extended state or larger swelling state, resulting in a looser micellar structure and greater DOX release [45]. Meanwhile, this electrostatic repulsion, together with the slight protonation of azobenzene groups mentioned above also triggers greater tension or instability on the hydrophobic cavity and Azo-PCL core, thus weakening the host-guest interaction between Azo and β-CD and facilitating the release of more DOX from the inner core of the supramolecular micelles [42]. In addition, under acidic conditions, the re-protonation of the amino groups of DOX increases the solubility of DOX in aqueous solution, and even the micelle cores degrade faster, resulting in the rapid release of DOX [47]. When the UV light irradiation is exerted in acidic environments at a pH of 5.0, the synergistic effect triggered by pH and UV light further accelerates the DOX release, offering a higher DOX release amount of approximately 89.8 % than that resulting from the single stimulus after a 30 h release. These properties provide the opportunity for the targeted and controlled release of DOX based on various physiological environments.

3.5 *In vitro* cytotoxicity assay

The MTT assay was conducted to determine the *in vitro* cytotoxicity of the blank supramolecular micelle and DOX-loaded micelle nanoparticles, DOX-β-CD-g-PDMAEMA@Azo-PCL, against HeLa cells in various environments, as demonstrated in Figure 6(B). It is clear that there is no significant difference in relative cell viability for the blank and DOX-loaded supramolecular micelles, and the cell survival rate is above 82% even at a high micelle concentration of 250 $mg \cdot L^{1}$ after cultivation in PBS at a pH of 7.4 for 24 h. Especially of note is that the value reaches up to 90% for the blank supramolecular micelles. Therefore, the as-prepared supramolecular assembly as a drug carrier is noncytotoxic, and the drug-loaded micelles can also be safely used to deliver DOX without harm to normal cells. In view of the small amount of DOX release from the DOX-loaded micelles under experimental conditions, it is reasonable that a slightly lower cell viability occurs for the drug-loaded micelles in comparison with the blank micelles. Free DOX, however, shows an obvious cell inhibition rate with a half maximal inhibitory concentration (IC_{50}) of approximately 2.87 μg mL^{-1}; this substantially affects cell metabolism and thus causes harm to normal cells. To value the anticancer activity of DOX-loaded supramolecular micelles, the cytotoxicity of the blank supramolecular assembly micelles with different concentrations was first assessed by culturing HeLa cells with blank micelles in PBS at a pH of 5.0 for 24 h and UV irradiation for 10 s, as shown in Figure S8 (SI). The results signify that the cytotoxicity is independent of the pH, momentary UV irradiation and micelle concentration and that their effects on cell growth can be negligible. This finding is in agreement with those reported elsewhere [48]. On this basis, HeLa cells seeded in a 96-well plate at a density of 1×10^{4} $well^{-1}$ were incubated in a 200 μl of fresh

DMEM medium containing the DOX-loaded supramolecular micelles adjusted to a pH of 5.0 for another 24 h and at the same time under UV irradiation for 10 s, giving the cytotoxicity results in Figure 6(B). Obviously, there is only approximately 8% cell survival with the 250 mg L^{-1} DOX-loaded supramolecular micelles, which have comparable and even superior anticancer activity to free DOX. This high anticancer activity is closely correlated with the fast cellular specific targeted release of DOX triggered by pH and UV irradiation, as shown in Figure 6(A). Therefore, the drug-loaded supramolecular micelles not only do not harm normal cells but also inhibit the growth of cancer cells *via* their unique photo- and pH-responsive properties in cellular drug release. The developed supramolecular self-assembly can therefore be potentially used as a DOX controlled release carrier for effective cancer therapy.

4. Conclusion

In conclusion, novel β-CD-g-PDMAEMA@Azo-PCL supramolecular polymers have been designed and synthesized via the host-guest interactions between β-CD and azobenzene, as confirmed by FTIR, (2D NOESY) ^{1}H NMR, LLS-GC, etc. The pH phase transition point of the supramolecular polymers is approximately 6.6, and the supramolecular micelles will reversibly self-assemble and dissociate under the alternating irradiation of ultraviolet and visible light. By changing the host/guest ratio and pH environment, the size and morphology of the micelles show regular changes. The supramolecular polymers are nontoxic and can encapsulate DOX, forming high-entrapment-efficiency supramolecular drug-loaded micelles that have obvious photo and pH response properties, which thus assume remarkable anticancer activity. An acidic environment and/or continuous ultraviolet light exposure significantly

accelerate the drug release rate. Therefore, they can have a potential application value in the fields of stimuli-responsive intelligent materials and nanobiomedicine.

Acknowledgments

This work is supported by the National Natural Science Foundation of China (grant 21572123 and 21773149) and the Fundamental Research Funds for the Central Universities (GK201601003).

Supporting Information

The Supporting Information is available.

- ^{1}H NMR and ^{13}C NMR spectra of β-CD, β-CD-Br, β-CD-*g*-PDMAEMA, Azo-OH and Azo-PCL; FT-IR spectra of β-CD, β-CD-Br, β-CD-*g*-PDMAEMA, Azo-OH and Azo-PCL; UV-vis spectra of Azo-PCL at various pH values; cytotoxicity of the blank supramolecular micelles under acidic and UV irradiation.

References

[1] Yang, L.; Tan, X.; Wang, Z.; Zhang, X. Supramolecular polymers: Historical development, preparation, characterization, and functions. *Chem. Rev.* 2015, 115, 7196−7239.

[2] Ma, X.; Zhao, Y. Biomedical applications of supramolecular systems based on host–guest interactions. *Chem. Rev.* 2015, 115, 7794–7839.

[3] Loh, X.J. Supramolecular host–guest polymeric materials for biomedical

applications. *Mater. Horiz.* 2014, 1, 185–195.

[4] Ma, X.; Tian, H. Stimuli-responsive supramolecular polymers in aqueous solution. *Acc. Chem. Res.* 2014, 47, 1971–1981.

[5] Hu, J.; Liu, S. Engineering Responsive Polymer Building Blocks with Host–Guest Molecular Recognition for Functional Applications. *Acc. Chem. Res.* 2014, 47, 2084–2095.

[6] Hu, Q.D.; Tang, G.P.; Chu, P.K. Cyclodextrin-based host-guest supramolecular nanoparticles for delivery: From design to applications. *Acc. Chem. Res.* 2014, 47, 2017–2025.

[7] Crini, G. Review: A histry of cyclodextrin. *Chem. Rev.* 2014, 10940–10975.

[8] Kang, Y.; Ma, Y.; Zhang, S.; Ding, L.; Li, B. Dual-stimuli-responsive nanoassemblies as tunable releasing carriers. *ACS Macro Lett*. 2015, 4, 543–547.

[9] Gao, C.; Liu, M.; Lv, S.; Zhang, X.; Duan, H. Fluorescent and thermoresponsive supramolecular systems: synthesis, self-assembly and application in percutaneous optical monitoring. *J. Mater. Chem. B* 2014, 2, 6823–6829.

[10] Yu, G.; Zhao, X.; Zhou, J.; Mao, Z.; Huang, X.; Wang, Z.; Hua, B.; Liu, Y.; Zhang, F.; He, Z.; Jacobson, O.; Gao, C.; Wang, W.; Yu, C.; Zhu, X.; Huang, F.; Chen, X. Supramolecular polymer-based nanomedicine: high therapeutic performance and negligible long-term immunotoxicity. *J. Am. Chem. Soc.* 2018, 140, 8005–8019.

[11] Hao, S.; Zhai, Q.; Zhao, L.; Xu, B. Construction and reversible assembly of a redox-responsive supramolecular cyclodextrin amphiphile. *Colloid Surf. A* 2016, 509, 116–122.

[12] Wang, Y.; Luo, Y.L.; Xu, F.; Chen, Y.S.; Tang, W. Redox-responsive PAEFc-*b*-PDMAEMA amphiphilic block copolymer self-assembly micelles:

physicochemical properties and anticancer drug controlled release. *J. Ind. Eng. Chem.* 2017, 48, 66–78.

[13] Zhou, J.; Xu, H.; Tong, Z.; Yang, Y.; Jiang, G. Photo/pH-controlled host-guest interaction between an azobenzene-containing block copolymer and water-soluble pillar[6]arene as a strategy to construct the "compound vesicles" for controlled drug delivery. *Mater. Sci. Eng. C* 2018, 89, 237–244.

[14] Guo, H.; Yang, J.; Zhou, J.; Zeng, L.; Zhao, L.; Xu, B. Photoresponsive self-assembly of a β-cyclodextrin derivative with an azobenzene terminal group in water. *Dyes Pigments* 2018, 149, 626–632.

[15] Lu, Y.; Zou, H.; Yuan, H.; Gu, S.; Yuan, W.; Li, M. Triple stimuli-responsive supramolecular assemblies based on host-guest inclusion complexation between β-cyclodextrin and azobenzene. *Eur. Polym. J.* 2017, 91, 396–407.

[16] Tong, Z.; Wang, R.; Huang, J.; Xu, J.; Fan, Z. Regulation of the self-assembly morphology of azobenzene-bearing double hydrophobic block copolymers in aqueous solution by shifting the dynamic host-guest complexation. *Polym. Chem.* 2015, 6, 2214–2225.

[17] Yang, L.; Lei, M.; Zhao, M.; Yang, H.; Zhang, K.; Zhang, H.; Li, Y.; Lei, Z. Synthesis of supramolecular polymer based on noncovalent "host–guest" inclusion complexation and its reversible self-assembly. *New J. Chem.* 2016, 40, 6825–6833.

[18] Mei, X.; Yang, S.; Chen, D.; Li, N.; Li, H.; Xu, Q.; G, J.; Lu, J. Light-triggered reversible assemblies of azobenzene-containing amphiphilic copolymer with β-cyclodextrin-modified hollow mesoporous silica nanoparticles for controlled drug release. *Chem. Commun.* 2012, 48, 10010–10012.

[19] Chen, C.; Zhao, J.; Gao, M.; Meng, X.; Fan, A.; Wang, Z.; Zhao, Y. Photo-triggered

micelles: simultaneous activation and release of microtubule inhibitors for on-demand chemotherapy. *Biomater. Sci.* 2018, 6, 511–518.

[20] Liu, D.; Wang, S.; Xu, S.; Liu, H. Photocontrollable intermittent release of doxorubicin hydrochloride from liposomes embedded by azobenzene-contained glycolipid. *Langmuir* 2017, 33, 1004–1012.

[21] Wang, W.; Lin, L.; Ma, X.; Wang, B.; Liu, S.; Yan, X.; Li, S.; Tian, H.; Yu, X. Light-induced hypoxia-triggered living nanocarriers for synergistic cancer therapy. *ACS Appl. Mater. Interfaces* 2018, 10, 19398–19407.

[22] Gao, Z.; Chen, M.; Hu, Y.; Dong, S.; Cui, J.; Hao, J. Tunable assembly and disassembly of responsive supramolecular polymer brushes. *Polym. Chem.* 2017, 8, 2764–2772.

[23] Bian, Q.; Wang, W.; Wang, S.; Wang, G. Light-triggered specific cancer cell release from cyclodextrin/azobenzene and aptamer-modified Substrate. *ACS Appl. Mater. Interfaces* 2016, 8, 27360−27367.

[24] Yang, F.; Cao, Z.; Wang, G. Micellar assembly of a photo- and temperature responsive amphiphilic block copolymer for controlled release. *Polym. Chem.* 2015, 6, 7995–8002.

[25] Dan, Z.; Cao, H.; He, X.; Zeng, L.; Zou, L.; Shen, Q.; Zhang, Z. Biological stimuli-responsive cyclodextrin-based host-guest nanosystems for cancer therapy. *Int. J. Pharm.* 2015, 483, 63–68.

[26] Li, L.; Lu, B.; Fan, Q.; Wei, L.; Wu, J.; Hou, J.; Guo, X.; Liu, Z. Synthesis and pH-responsive self-assembly behavior of a fluorescent amphiphilic triblock copolymer mPEG-*b*-PCL-*b*-PDMAEMA-g-PC for the controlled intracellular delivery of doxorubicin. *RSC Adv.* 2016, 6, 27102–27112.

[27] Zhang, M.; Xiong, Q.; Chen, J.; Wang, Y.; Zhang, Q. A novel cyclodextrin-containing pH-responsive star polymer for nanostructure fabrication and drug delivery. *Polym. Chem.* 2013, 4, 5086–5095.

[28] Xiong, Q.; Zhang, M.; Zhang, Z.; Shen, W.; Liu, L.; Zhang, Q. Anti-tumor drug delivery system based on cyclodextrin-containing pH-responsive star polymer: *in vitro* and *in vivo* evaluation. *Int. J. Pharm.* 2014, 474, 232–240.

[29] Behzadi, S.; Gallei, M.; Elbert, J.; Appold, M.; Glasser, G.; Landfester K.; Crespy, D. A triblock terpolymer *vs.* blends of diblock copolymers for nanocapsules addressed by three independent stimuli. *Polym. Chem.* 2016, 7, 3434–3443.

[30] Kellum, M.G.; Smith, A.E.; York, S.K.; McCormick, C.L. Reversible interpolyelectrolyte shell cross-linked micelles from pH/salt-responsive diblock copolymers synthesized *via* RAFT in aqueous solution. *Macromolecules* 2010, 43, 7033–7040.

[31] Rakhmatullina, E.; Meier, W. Solid-supported block copolymer membranes through interfacial adsorption of charged block copolymer vesicles. *Langmuir* 2008, 24, 6254-6261.

[32] Zhou, Z.; Guo, F.; Wang, N.; Meng, M.; Li, G. Dual pH-sensitive supramolecular micelles from star-shaped PDMAEMA based on β-cyclodextrin for drug release. *Int. J. Biol. Macromol.* 2018, 116, 911–919.

[33] Liu, X.; Ni, P.; He, J.; Zhang, M. Synthesis and Micellization of pH/temperature-responsive double-hydrophilic diblock copolymers polyphosphoester-*block*-poly[2-(dimethylamino)ethyl methacrylate] prepared *via* ROP and ATRP. *Macromolecules* 2010, 43, 4771–4781.

[34] Zhang, P.; Qian, X. P.; Zhang, Z. K.; Li, C.; Xie, C.; Wu, W.; Jiang, X. Q.

Supramolecular amphiphilic polymer-based micelles with seven-armed polyoxazoline coating for drug delivery. *ACS Appl. Mater. Interfaces* 2017, 9, 5768−5777.

[35] Shen, P.; Qiu, L. Dual-responsive recurrent self-assembly of a supramolecular polymer based on the host-guest complexation interaction between β-cyclodextrin and azobenzene. *New J. Chem.* 2018, 42, 3593–3601.

[36] Fang, L.; Li, Y.; Chen, Z.; Liu, W.; Zhang, J.; Xiang, S.; Shen, H.; Li, Z.; Yang, B. Tunable polymer brush/Au NPs hybrid plasmonic arrays based on host−guest interaction. *ACS Appl. Mater. Interfaces* 2014, 6, 19951−19957.

[37] [c] Zhao, Y.; Guo, K.; Wang, C.; Wang, L. Effect of inclusion complexation with cyclodextrin on the cloud point of poly(2-(dimethylamino)ethyl methacrylate) solution. *Langmuir* 2010, 26(11), 8966–8970.

[38] Yu, Y.; Sun, X.; Zhang, R.; Yuan, S.; Lu, Q.; Wu, Z. Synthesis and properties of amphiphilic thermo-sensitive block copolymers. *J. Polym. Res.* 2017, 24, 55.

[39] Yuan, W.; Shen, J.; Guo, W. Thermoresponse and light-induced reversible self-assembly/disassembly of supra-amphiphiles from azobenzene and β-cyclodextrin-containing copolymers. *Mater. Lett.* 2014,134, 259–262.

[40] Zou, H.; Lu, Y.; Yuan, W.; Wang, S. UV light- and thermo-responsive hierarchical assemblies based on the inclusion complexation of β-cyclodextrin and azobenzene. *Polym. Chem.* 2017, 8, 661–665.

[41] Dhammika Bandara, H. M.; Burdette, S. C. Photoisomerization in different classes of azobenzene. *Chem. Soc. Rev.* 2012, 41, 1809–1825.

[42] Stubbs, E.; Laskowski, E.; Conor, P.; Heinze, D. A.; Karis, D.; Glogowski, E. M. Control of pH- and temperature-responsive behavior of mPEG-b-PDMAEMA

copolymers through polymer composition. *J. Macromol. Sci. A* 2017, 54, 228–235.

[43] Xiong, D.; Zhang, X.; Peng, S.; Gu, H.; Zhang, L. Smart pH-sensitive micelles based on redox degradable polymers as DOX/GNPs carriers for controlled drug release and CT imaging. *Colloid Surface B* 2018, 163, 29–40.

[44] Car, A.; Baumann, P.; Duskey, J.T.; Chami, M.; Bruns, N.; Meier, W. pH-Responsive PDMS-*b*-PDMAEMA micelles for intracellular anticancer drug delivery. *Biomacromolecules* 2014, 15, 3235–3245.

[45] Lei, Z.; Vaidyalingam, A.; Dutta, P.K. Photochemistry of azobenzene in microporous aluminophosphate $AlPO_4$-5. *J. Phys. Chem. B* 1998, 102, 8557–8562.

[46] Li, Z.; Tan, B. H. Towards the development of polycaprolactone based amphiphilic block copolymers: Molecular design, self-assembly and biomedical applications. *Mater. Sci. Eng. C* 2014, 45, 620–634.

[47] Shuai, X.; Ai, H.; Nasongkla, N.; Kim, S.; Gao, J. Micellar carriers based on block copolymers of poly(*q*-caprolactone) and poly(ethylene glycol) for doxorubicin delivery. *J. Control Rel.* 2004, 98, 415–426.

[48] Li, Q.; Yao, W.; Yu, X.; Zhang, B. Dong,; J.; Jin, Y. Drug-loaded pH-responsive polymeric micelles: Simulations and experiments of micelle formation, drug loading and drug release. *Colloid Surface B* 2017, 158, 709–716.